

Supporting Information for

CQDs Boosted Pd/TiO₂ for Enhanced Hydrogen Evolution via

Formaldehyde Reforming

Xiaogang Liu*, Wenjie Chen and Xin Zhang

*College of Chemistry and Chemical Engineering, Xinyang Normal University, Xinyang, Henan
464000, P. R. China.*

E-mail: lxg133298@163.com

Experimental Section

Chemical Reagents.

Ti(OC₄H₉)₄ (TBOT, 98.5%) was purchased from General Reagent, Ltd. PdCl₂ (99%), NaOH (98%) and HCHO (37-40% in water) were obtained from Adamas Reagent, Ltd. HF (40%) and NaBH₄ (98%) were bought from Sinopharm Chemical Reagent Co., Ltd. Deionized water was used in all experiments. All chemicals were of analytical reagent grade and used without further purification.

Synthesis of TiO₂.

TiO₂ nanosheets were prepared by a hydrothermal method.¹ Specifically, 6 mL of HF solution was dropped into a dry Teflon liner containing 25 mL of TBOT and stirred for 30 min. Then the mixture was transferred to an autoclave and hydrothermally treated at 180 °C for 24 h. The white precipitate was collected by centrifugation and washed with ethanol and deionized water several times and dried in an oven at 60 °C for 12 h to obtain TiO₂ nanosheets (for convenience, denoted as TiO₂).

Synthesis of CQDs.

Carbon quantum dots (CQDs) were prepared according to the reported literature.² Typically, 3 g of glucose was added into 40 mL of deionized water to obtain transparent solution. The mixed solution was then transferred into 50 mL of Teflon-lined stainless steel autoclave and heated at 160°C for 0.5 h. After the reaction, the suspension was centrifuged to remove the precipitates. The supernatant was filtered through a Teflon membrane, and the filtrate was treated with a 1000 Da dialysis bag for 7 days. The as-obtained solution was denoted as CQDs solution and further used to prepare other catalysts.

Synthesis of CQDs/TiO₂.

0.4 g of TiO₂ powder was dispersed in 20 mL of deionized water with continuous stirring for 0.5 h. Then 172 μL of CQDs (ca. 46.47 mg/mL) solution was dropped into the above suspension and stirred for 2 h. After that, the suspension was transferred to Teflon autoclave and kept at 120 °C for 4 h. Finally, the CQDs/TiO₂ powders were obtained by centrifugation, washing with ethanol and water for 4 times and drying in an oven at 60 °C.

Synthesis of Pd/CQDs/TiO₂.

0.2 g of CQDs/TiO₂ powder was uniformly dispersed in a mixed solution containing 30 mL of deionized water and 10 mL of ethanol. Then, an appropriate amount of PdCl₂ solution was added to the above homogeneous solution. After stirring for 10 min, 10 mL freshly prepared NaBH₄ (0.5 M) aqueous solution was added. After 6 h of reaction at room temperature, the solid precipitate was centrifuged, washed with ethanol and deionized water several times, and dried at 60°C for 12 h. The samples were denoted as Pd/CQDs/TiO₂-x% (x=0.5, 1, 3 and 5), where 'x' represented the theoretical mass ratio of Pd to CQDs/TiO₂.

Characterizations.

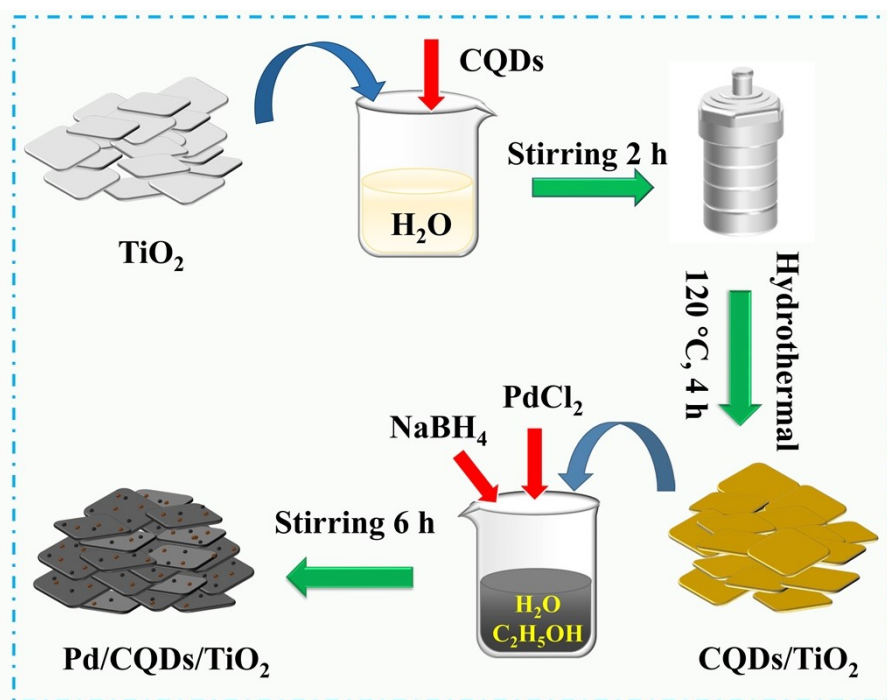
The morphologies of the samples were observed by field-emission scanning electron microscopy (FE-SEM, S-4800, Hitachi). The microstructure of Pd/CQDs/TiO₂ was acquired by using FEI Tecnai G2 F20 transmission electron microscopy (TEM). The crystals of the catalysts were recorded on a Rigaku Mini Flex 600 X-ray diffraction (XRD) with a scan range of 20–90°, a scan speed of 10 °/min. The catalyst surface information was collected by K-Alpha 0.5eV X-ray photoelectron spectroscopy (XPS) using Al-K α radiation as the excitation source and standard C 1s (284.8 eV) as a reference for calibrating other elements. The exact loadings of Pd in the samples were determined by inductively coupled plasma mass spectrometry (ICP-MS, Agilent 8900). Fourier Transform Infrared (FTIR) spectra were monitored by a Thermo Scientific Nicolet iS50 spectrometer. The specific surface area and pore size distribution of the synthesized materials were determined by nitrogen adsorption/desorption method using a Micro-Meritic ASAP 2460 specific surface area and pore size analyzer. Raman spectra were recorded with a LabRAM HR instrument at an excitation wavelength of 532 nm. Electron paramagnetic resonance (EPR) signals were recorded on a Bruker EPR A-300 spectrometer. The EPR signals of free radicals generated during the HCHO-reforming process were trapped by 5, 5-dimethyl-1-pyrroline N-oxide (DMPO) at room temperature.

Hydrogen evolution experiment.

In the catalytic hydrogen production process, 15 mg of catalyst was uniformly dispersed in a pre-configured bottle containing a certain amount of NaOH solution under magnetic agitation. Then, a certain volume of formaldehyde solution was added to the reactor and sealed the

vessel immediately while the hydrogen production reaction began immediately. Every 5 min, 150 μL of mixed gas was extracted and injected into a gas chromatograph (GC) equipped with a TCD detector and argon as carrier gas. Only H_2 and no other gases were analyzed during the reaction. The chromatogram was calibrated with pure hydrogen (99.999%) by external standard method, the standard curves of hydrogen production (V, mL) versus chromatographic peak area (S) is as follows:

$$V (\text{mL}) = 3.6021 \times 10^{-5} S + 12.51$$



Scheme S1. Schematic preparation of Pd/CQDs/TiO₂.

Additional discussion:

The preparation of the Pd/CQDs/TiO₂ underwent two steps of hydrothermal and impregnation-reduction process, as illustrated in Scheme S1. Firstly, the prepared TiO₂ nanosheets and CQDs solution were mixed and hydrothermally reacted to prepare CQDs/TiO₂. Subsequently, the CQDs/TiO₂ catalyst was dipped in palladium chloride solution and reduced by sodium borohydride to prepare Pd/CQDs/TiO₂. The detailed preparation process is shown in the experimental section.

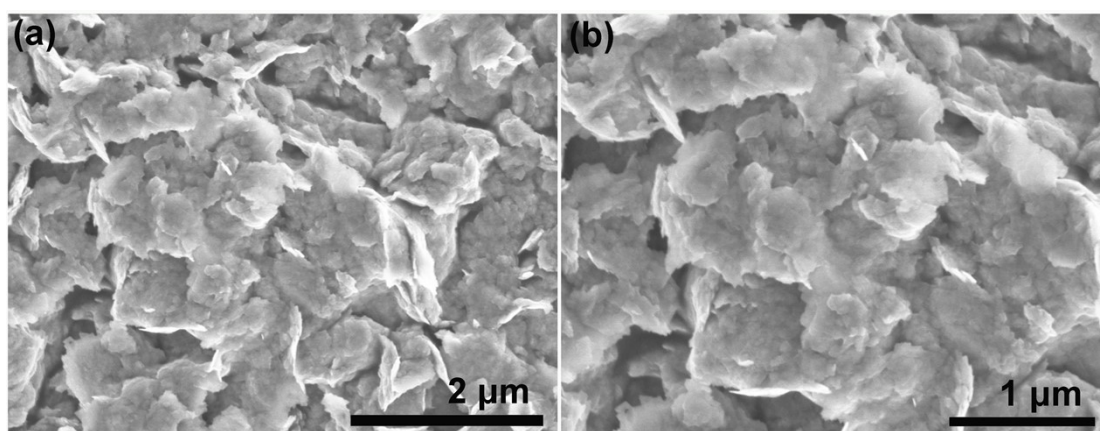


Figure S1. (a, b) SEM images of TiO₂.

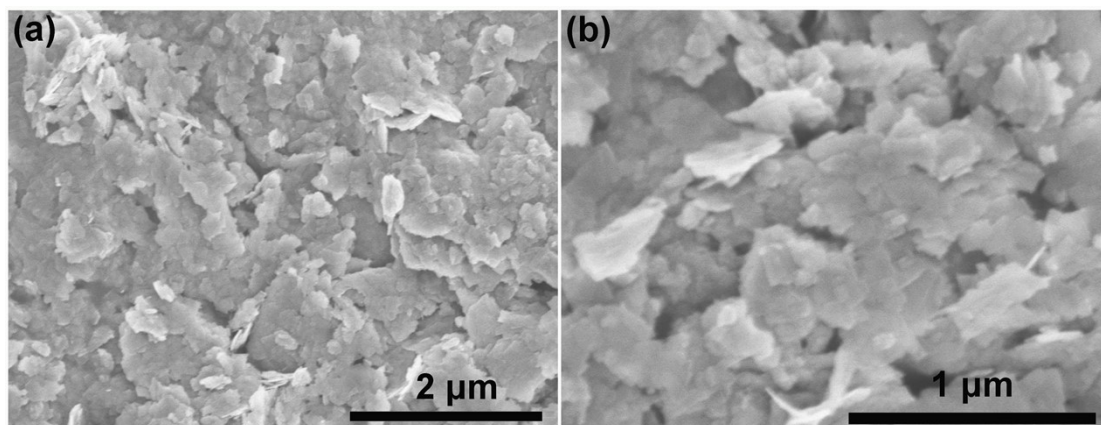


Figure S2. (a, b) SEM images of CQDs/TiO₂.

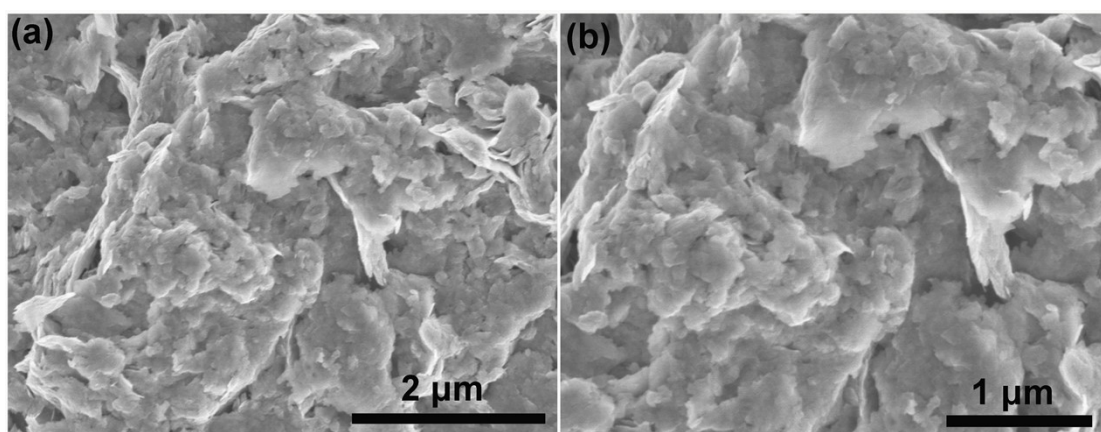


Figure S3. (a, b) SEM images of Pd/TiO₂-3%.

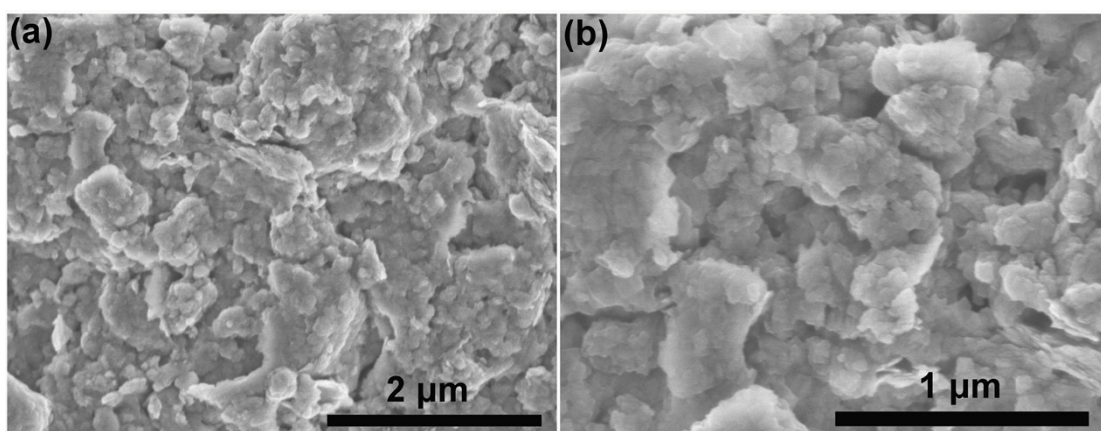


Figure S4. (a, b) SEM images of Pd/CQDs/TiO₂-3%

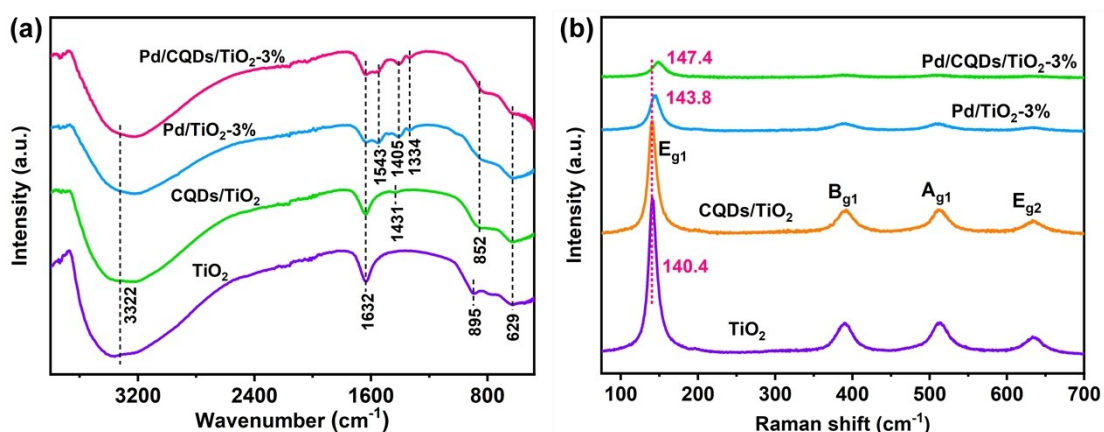


Figure S5. (a) FT-IR spectra and (b) Raman spectra of TiO₂, CQDs/TiO₂, Pd/TiO₂-3% and Pd/CQDs/TiO₂-3%.

Additional discussion: For pristine TiO₂, the broad band observed at 3322 cm⁻¹ corresponds to the stretching vibration of the hydroxyl group (O-H) of TiO₂ nanosheets. The band at 1632 cm⁻¹ is attributed to the bending vibration peak TiO₂-OH of surface absorbed water. Moreover, two weak bands located at 895 and 629 cm⁻¹ for TiO₂ correspond to the Ti-O-Ti and Ti-O-C vibrations.³ In the case of CQDs/TiO₂, a new band at 1431 cm⁻¹ associated with the vibration of C=O group is also found, which is the characteristic peak of CQDs. Compared with pure TiO₂, the band representing the Ti-O-Ti stretching vibration of CQDs/TiO₂ is blue-shifted to 852 cm and the band intensity of Ti-O-C is slightly enhanced. The hydroxyl could react with C=O bond of CQDs to form Ti-O-C bonds. These results demonstrate CQDs have been decorated on TiO₂ substrate, as well as the interaction between CQDs and TiO₂. In addition to the above bands, characteristics of surface adsorbed carbonate are also observed for Pd/TiO₂ and Pd/CQDs/TiO₂-3% samples, of which the bands at 1543, 1405 and 1334 cm⁻¹ correspond to asymmetric or symmetric stretching vibrational mode of $\nu_{as}(\text{CO}_3)$, $\nu_s(\text{CO}_3)$ (monodentate) and $\nu_{as}(\text{CO}_3)$ (bidentate), respectively.⁴ The Raman spectra are shown in Figure S5b. Four distinct peaks corresponding to characteristics of TiO₂ are observed at 140.4, 390.6, 512.2, and 635.3 cm⁻¹ for TiO₂ and CQDs/TiO₂, which are attributed to E_{g1}, B_{g1}, A_{g1} and E_{g2} bands of anatase TiO₂, respectively.⁵ A slight shift of E_{g1}-band towards higher wavenumber observed on Pd/TiO₂ and Pd/CQDs/TiO₂-3% indicates strong chemical bonding and electron interaction between Pd NPs and TiO₂ nanosheets.

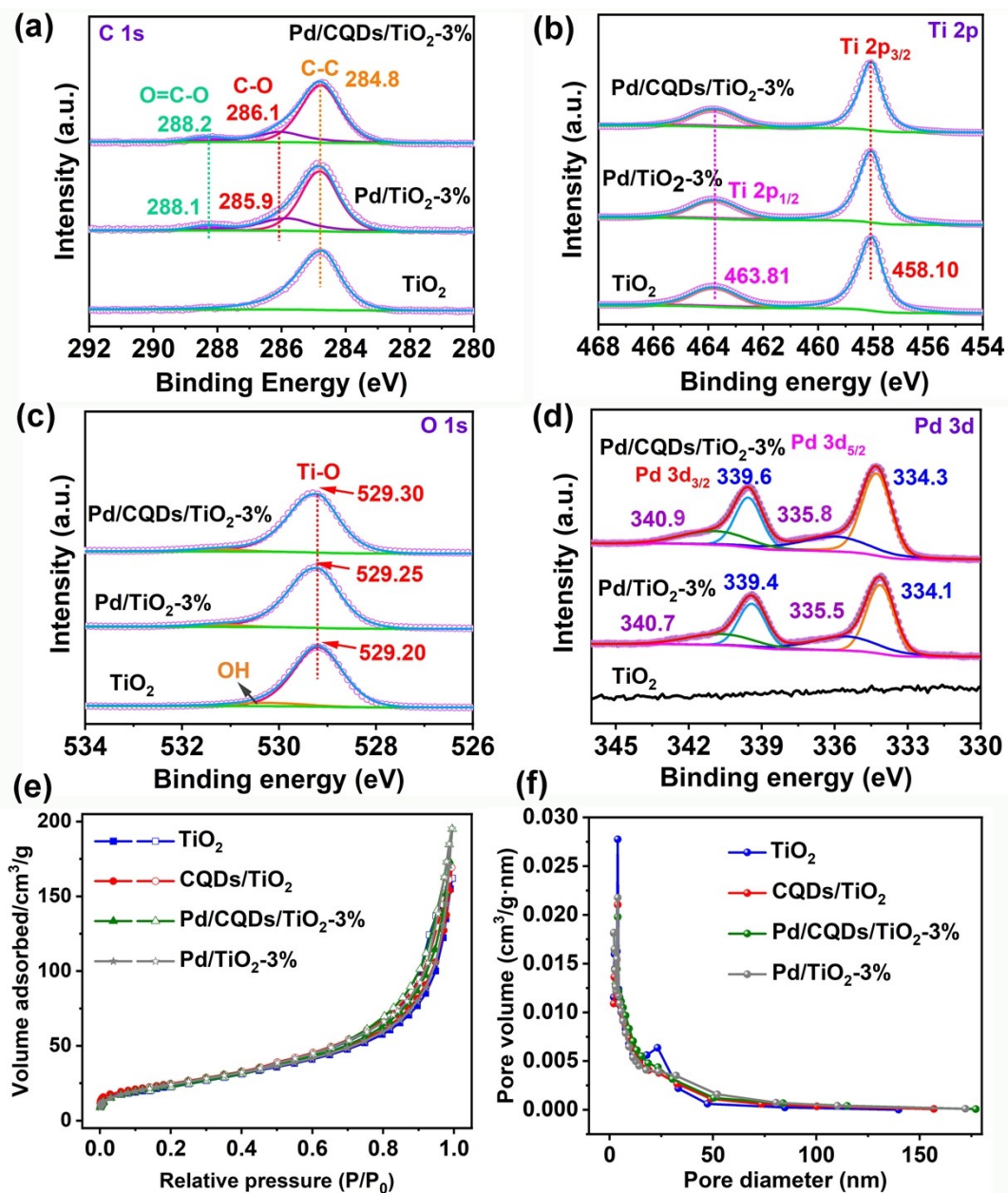


Figure S6. (a) C 1s, (b) Ti 2p, (c) O 1s and (d) Pd 3d XPS spectra; (e) N₂ adsorption/desorption isotherms and (f) the corresponding pore size distribution curves of prepared catalysts.

Table S1 Textural information of prepared samples.

Samples	S _{BET} /(m ² • g ⁻¹)	Pore volume /(cm ³ •g ⁻¹)	Pore diameter / nm
TiO ₂	85.48	0.26	7.33
CQDs/TiO ₂	89.92	0.28	7.46
Pd/CQDs/TiO ₂ - 0.5%	96.65	0.30	8.08
Pd/CQDs/TiO ₂ -1%	91.80	0.30	8.23
Pd/CQDs/TiO ₂ -3%	90.22	0.32	8.04
Pd/CQDs/TiO ₂ -5%	94.99	0.34	8.04
Pd/ TiO ₂ -3%	89.70	0.32	7.36

Table S2. Analysis for ICP-AES results of prepared samples.

Samples	Pd contents (wt. %)
Pd/CQDs/TiO ₂ -0.5%	0.68
Pd/CQDs/TiO ₂ -1%	0.87
Pd/CQDs/TiO ₂ -3%	2.34
Pd/CQDs/TiO ₂ -5%	3.58
Pd/TiO ₂ -0.5%	2.47

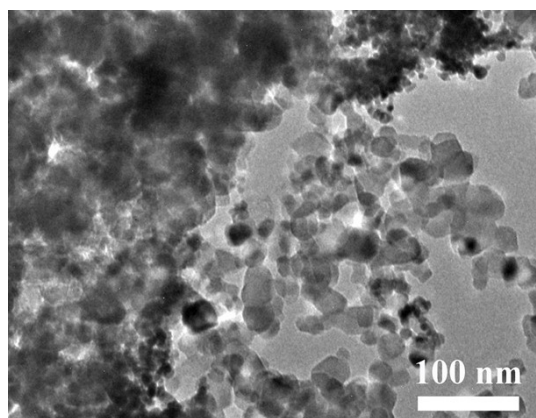


Figure S7. TEM image of Pd nanoparticles prepared by NaBH_4 reduction.

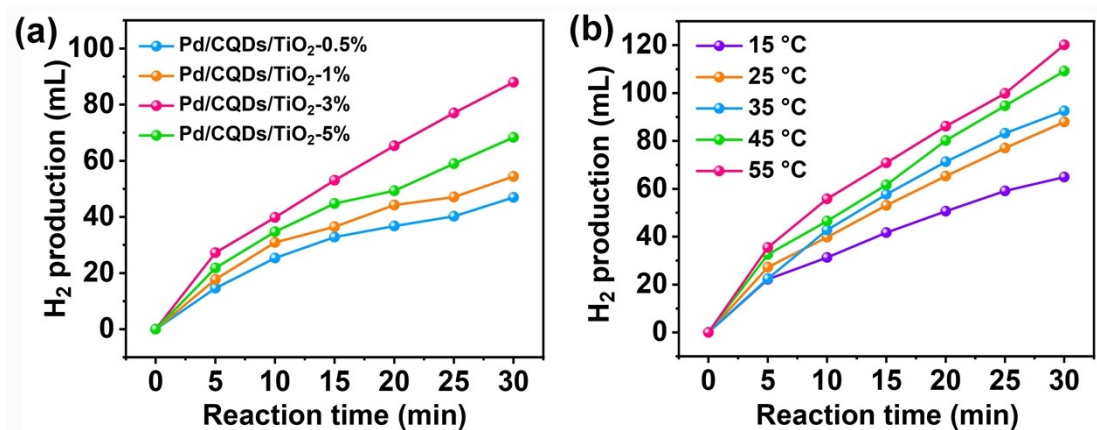


Figure S8. The effects of (a) Pd loading and (b) reaction temperature on the H_2 production as a function of reaction time.

Additional discussions

The catalytic performance of Pd/TiO₂ catalysts with different Pd loadings shows that the hydrogen production is the highest when the Pd loading is 3 wt% (Figure S8a). Although the elevated temperature is beneficial for H_2 production, too high temperature increases the cost of hydrogen production and is detrimental to the stability of the catalyst (Figure S8b). Thus, the reaction temperature was fixed at room temperature of 25°C.

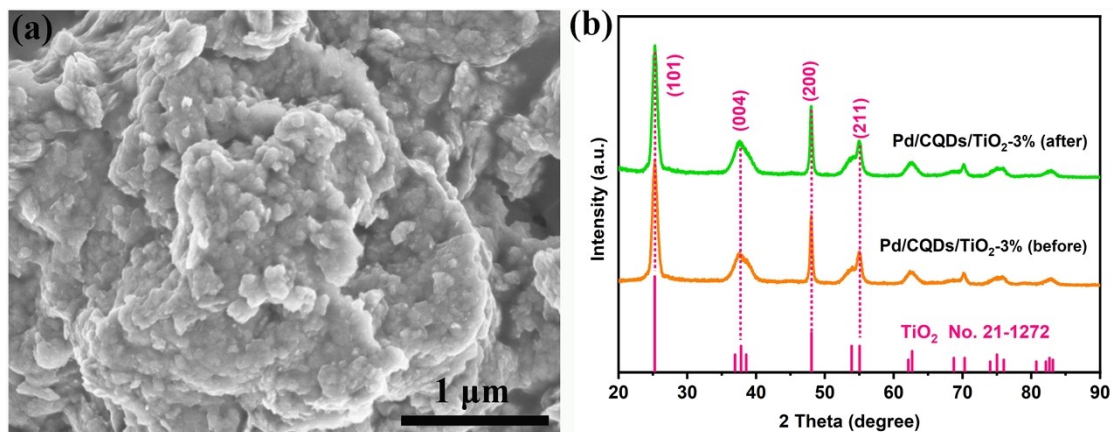


Figure S9. (a) SEM images of Pd/CQDs/TiO₂-3% after catalytic reaction. (b) XRD patterns of Pd/CQDs/TiO₂-3% before and after catalytic H₂ production.

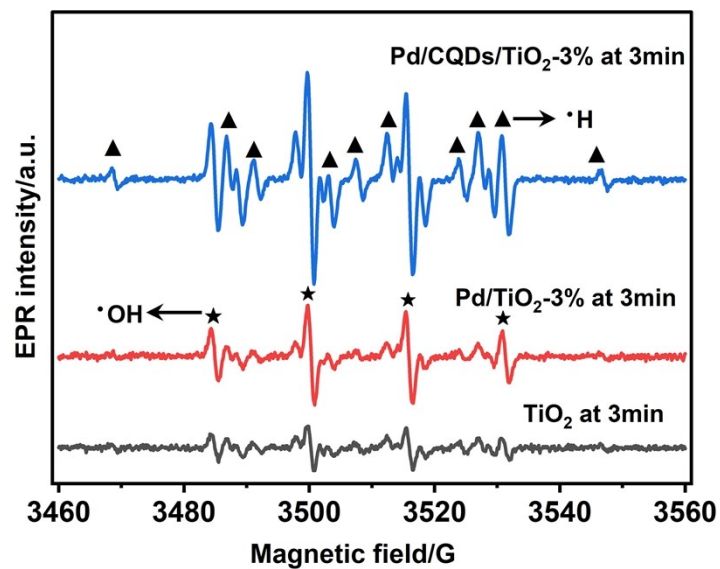


Figure S10. DMPO adducts recorded for TiO₂, Pd/TiO₂ and Pd/CQDs/TiO₂-3% after reaction in alkaline aqueous solution (1 M NaOH) for 3 min.

Additional discussions

To further clarify the effects of CQDs in Pd/CQDs/TiO₂ on the hydrogen production performance, the DMPO trapped EPR spectra in alkaline water solution (1 M of NaOH) for TiO₂, Pd/TiO₂-3%

and Pd/CQDs/TiO₂-3%. As shown in Figure S10, traces of DMPO-•H ($A_N=16.7$ G, $A_{H1}=A_{H2}=22.5$ G) and DMPO-•OH ($A_N=A_H=16.2$ G) complexes are detected in the suspension containing TiO₂ and alkaline water solution, indicating water dissociation can occur on the surface of TiO₂. In Pd/TiO₂-3%, large amount of DMPO-•H and DMPO-•OH are detected, indicating the introduction of Pd species are more favorable for the water dissociation. Moreover, the intensity of the DMPO-•H and DMPO-•OH is notably enhanced after the introduction of CQDs in Pd/TiO₂-3% composite, which further implies that the synergy between Pd and CQDs in dynamically promoting the water dissociation. Thus, the preferable water dissociation reaction of Pd/CQDs/TiO₂-3% is beneficial to promote the subsequent proton coupling reaction, thereby improving its hydrogen production performance in aqueous HCHO solution.

1. J. G. Yu, J. X. Low, W. Xiao, P. Zhou and M. Jaroniec, *Journal of the American Chemical Society*, 2014, **136**, 8839-8842.
2. J. J. Zhu, H. Y. Yin, Z. Z. Cui, D. Y. Qin, J. Y. Gong and Q. L. Nie, *Appl. Surf. Sci.*, 2017, **420**, 323-330.
3. Y. Sui, L. Wu, S. Zhong and Q. Liu, *Appl. Surf. Sci.*, 2019, **480**, 810-816.
4. C. Zhang, F. Liu, Y. Zhai, H. Ariga, N. Yi, Y. Liu, K. Asakura, M. Flytzani-Stephanopoulos and H. He, *Angewandte Chemie International Edition*, 2012, **51**, 9628-9632.
5. F. Tian, Y. Zhang, J. Zhang and C. Pan, *The Journal of Physical Chemistry C*, 2012, **116**, 7515-7519.